Acta Crystallographica Section C
Crystal Structure Communications
ISSN 0108-2701

A non-twinned polymorph of $\mathrm{CaTe_2O_5}$ from a hydrothermally grown crystal

Matthias Weil* and Berthold Stöger

Institute for Chemical Technologies and Analytics, Division of Structural Chemistry, Vienna University of Technology, Getreidemarkt 9/164-SC, A-1060 Vienna, Austria
Correspondence e-mail: mweil@mail.zserv.tuwien.ac.at

Received 30 July 2008
Accepted 2 August 2008
Online 9 August 2008

In contrast with the multiple twinning and/or domain formation found in the mica-like polymorphs of $\mathrm{CaTe_2O_5}$, calcium pentaoxidoditellurate(IV), that have been prepared by solid-state reactions and for which complete structure determinations have not been successful up to now, the crystal structure of a hydrothermally grown phase was fully determined from a non-twinned crystal. The structure is made up of alternating layers of $\mathrm{Ca^{2+}}$ cations and of $_{\infty}^{2}[\mathrm{Te_2O_5}]^{2-}$ anions stacked along [100]. The lone-pair electrons E of the $\mathrm{Te^{IV}}$ atoms are stereochemically active and protrude into channels within the anionic layer. In comparison with analogous $M^{\mathrm{II}}\mathrm{Te_2O_5}$ structures (M = Mg, Mn, Ni or Cu) with ditellurate(IV) anions that are exclusively made up of corner-sharing TeO_x (x = 3–5) polyhedra resulting in flat $_{\infty}^{2}[\mathrm{Te_2O_5}]^{2-}$ layers, the anionic layers in $\mathrm{CaTe_2O_5}$ are undulating and are built of corner- and edge-sharing $[\mathrm{TeO_4}]$ polyhedra.

Comment

The ditellurate(IV) $\mathrm{CaTe_2O_5}$ has been the subject of several previous investigations and can be prepared in polycrystalline form by heating stoichiometric amounts of the binary oxides above 800 K (Trömel & Ziethen-Reichnach, 1970). Single crystals of this material were grown by slow cooling of the melt through the melting point (965 K; Redman *et al.*, 1970) and they exhibit interesting ferroelectric properties over a wide temperature range (Sadovskaya *et al.*, 1983, 1987). However, multiple twinning and/or formation of domain structures in the mica-like crystals have prevented a complete structure determination so far (Trömel & Ziethen-Reichnach, 1970; Redman *et al.*, 1970; Gorbenko *et al.*, 1983). More recent thermal analysis studies of $\mathrm{CaTe_2O_5}$ (also prepared by solid-state reaction) revealed several phase transitions, with one room-temperature polymorph, denoted α-$\mathrm{CaTe_2O_5}$, and three high-temperature polymorphs (β, γ and δ) (Mishra *et al.*, 1998). The corresponding X-ray powder diffraction patterns of the different phases were indexed on the basis of monoclinic (α- and β-polymorphs), orthorhombic (γ-polymorph) and tetragonal (δ-polymorph) unit cells (Tripathi *et al.*, 2001), but for none of these phases were the structures solved. We have likewise obtained a compound with the composition $\mathrm{CaTe_2O_5}$ during hydrothermal treatment of phases in the system Ca–Te–O (see *Experimental*). Following the nomenclature of Mishra *et al.* (1998), this fifth $\mathrm{CaTe_2O_5}$ polymorph is accordingly denoted ε-$\mathrm{CaTe_2O_5}$.

The structure of ε-$\mathrm{CaTe_2O_5}$ contains one Ca, two Te and five O atoms in the asymmetric unit. The main building units of the structure are two different $[\mathrm{TeO_4}]$ polyhedra and one $[\mathrm{CaO_7}]$ polyhedron. The $[\mathrm{TeO_4}]$ polyhedra are linked by corner- and edge-sharing to build undulating layers with an overall composition of $_{\infty}^{2}[\mathrm{Te_2O_5}]^{2-}$ that propagate parallel to (100). Adjacent tellurate(IV) layers are interconnected by intermediate $\mathrm{Ca^{2+}}$ cations to establish a structure with alternating layers and a stacking sequence $\mathrm{Ca^{2+}}$ (at $x \simeq 0$)–$_{\infty}^{2}[\mathrm{Te_2O_5}]^{2-}$–$\mathrm{Ca^{2+}}$ (at $x \simeq 1$) along [100] (Fig. 1).

The two Te atoms are in oxidation state +IV and they are each surrounded by three O atoms at short Te—O distances of less than 2 Å. A fourth O atom situated at longer distances of 2.178 (5) (Te2) and 2.450 (5) Å (Te1), respectively, complements their coordination spheres (Table 1). In general, the O-atom coordination and coordination numbers of Te for various oxotellurates(IV) show great variation, with typical Te—O distances and coordination numbers in the ranges 1.8–2.35 Å and 3–5, respectively (Zemann, 1971). However, for saturation of the bond-valence sums, more remote O atoms up to Te—O distances of 2.60 Å should be considered as weakly bonding, giving rise to a [3+1] O-atom coordination for Te1 and a [4] O-atom coordination for Te2. The corresponding $[\mathrm{TeO_4}]$ polyhedra might be described as distorted trigonal bipyramids with one ligand occupied by the nonbonding lone-pair electrons E of the $\mathrm{Te^{IV}}$ atoms. As for the structures of other oxotellurate(IV) compounds (Zemann, 1971; Dolgikh, 1991), the stereochemical influence of the lone-pair electrons is obvious. They are situated opposite each other on the interior of the undulating oxotellurate(IV) layers and point towards the voids (Fig. 1). Due to the spiral arrangement of the condensed $[\mathrm{TeO_4}]$ polyhedra, these voids form channels that run parallel to [011] (Fig. 2) and [$0\bar{1}1$], with diameters of about 5 Å. Additional channels with a somewhat smaller diameter of

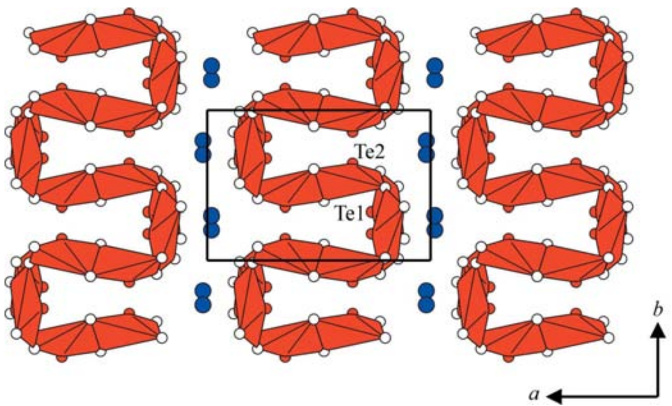

Figure 1
The crystal structure of ε-$\mathrm{CaTe_2O_5}$ in a projection along [001]. $[\mathrm{TeO_4}]$ polyhedra are shaded, Ca atoms are displayed as large filled spheres, Te atoms as small shaded spheres and O atoms as open spheres.

doi:10.1107/S0108270108024827

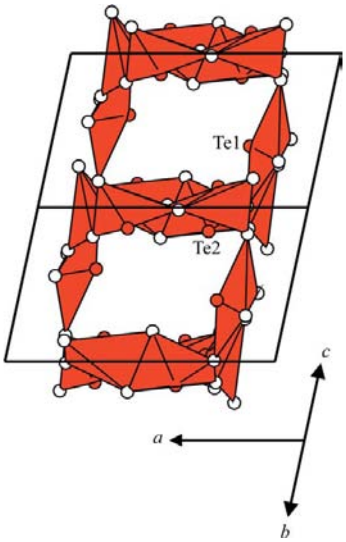

Figure 2
Channels in the ${}^{2}_{\infty}[\mathrm{Te_2O_5}]^{2-}$ layer (polyhedral description) extending parallel to [011]. The channels parallel to [0$\bar{1}\bar{1}$] are similar.

about 4.4 Å extend parallel to [$x \simeq \frac{1}{2}$, y, $z \simeq \frac{1}{4}$] and [$x \simeq \frac{1}{2}$, y, $z \simeq \frac{3}{4}$] (Fig. 3).

In comparison with the crystal structures of analogous $M^{\mathrm{II}}\mathrm{Te_2O_5}$ phases, where M^{II} = Mg (Weil, 2005) and the isotypic β-Mn (space group *Pbcn*; Johnston & Harrison, 2002), and the denningite-type α-Mn ($P4_2/nbc$; Miletich, 1993), Ni (*Pnma*; Platte & Trömel, 1981) and Cu ($P2_1/c$; Hanke *et al.*, 1973), the structural set-up of the anionic layers in ε-$\mathrm{CaTe_2O_5}$ is unique. When Te—O interactions of less than 2.60 Å are considered as bonding, the other $M^{\mathrm{II}}\mathrm{Te_2O_5}$ structures are similarly made up of layered ${}^{2}_{\infty}[\mathrm{Te_2O_5}]^{2-}$ anions (except for the columnar arrangement of $\mathrm{Te_2O_5}^{2-}$ anions in α-$\mathrm{MnTe_2O_5}$, where the shortest Te—O distance between adjacent columns is > 2.9 Å), with the lone-pair electrons protruding into the empty space of the structures. However, all these layers are flat and constructed solely from corner-sharing TeO_x (x = 3–5) polyhedra (Fig. 4), in contrast with ε-$\mathrm{CaTe_2O_5}$, with its undulating anionic layers composed of both corner- and edge-sharing [$\mathrm{TeO_4}$] polyhedra (Fig. 3).

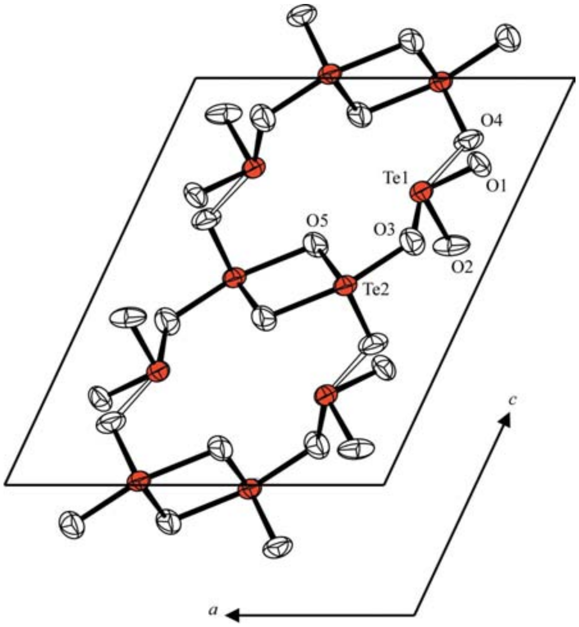

Figure 3
Part of the ${}^{2}_{\infty}[\mathrm{Te_2O_5}]^{2-}$ layer of ε-$\mathrm{CaTe_2O_5}$ in a projection along [010], showing the channels along [$x \simeq \frac{1}{2}$, y, $z \simeq \frac{1}{4}$] and [$x \simeq \frac{1}{2}$, y, $z \simeq \frac{3}{4}$]. Displacement ellipsoids are drawn at the 90% probability level. Short Te—O bonds of less than 2.20 Å are drawn with solid bonds, whereas the longer Te—O bond [2.450 (5) Å] is drawn with open bonds.

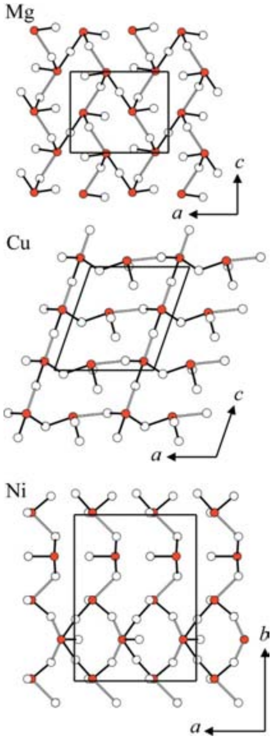

Figure 4
Construction of the ${}^{2}_{\infty}[\mathrm{Te_2O_5}]^{2-}$ layers in other $M^{\mathrm{II}}\mathrm{Te_2O_5}$ structures. The Te atoms are displayed as shaded spheres and the O atoms as open spheres. Short Te—O bonds of less than 2.20 Å are drawn with solid bonds and longer Te—O bonds are drawn with open bonds. Crystal data for M = Mg, Ni and Cu were taken from Weil (2005), Platte & Trömel (1981) and Hanke *et al.* (1973), respectively.

The Ca^{2+} cations form a distorted hexagonal layer parallel to (100) and they are bonded to seven O atoms from neighbouring anionic layers with Ca—O distances ranging from 2.305 (4) to 2.682 (5) Å, which compare well with those observed for $\mathrm{CaTeO_4}$ (Hottentot & Loopstra, 1979) or $\mathrm{Ca_4Te_5O_{14}}$ (Weil, 2004). Moreover, the average Ca—O distance of 2.44 Å is in very good agreement with the value of 2.42 Å calculated from the sum of the ionic radii for O^{2-} and seven-coordinate Ca^{2+} given by Shannon (1976).

The O atoms exhibit different coordination environments, with coordination numbers of 4 for O3 (2 × Ca and 2 × Te as coordination partners), 3 for O1, O2 (both 1 × Te and 2 × Ca) and O4 (1 × Ca and 2 × Te), and 2 for O5 which acts exclusively as the bridging atom between two $\mathrm{Te^{IV}}$ centres. Results from bond-valence sum (BVS) calculations (Brown, 2002), using the parameters of Brese & O'Keeffe (1991), are in accordance with expected values: Ca = 2.08 (expected 2.00), Te1 = 4.15 (4.00), Te2 = 4.13 (4.00), O1 = 2.15 (2.00), O2 = 2.20 (2.00), O3 = 2.16 (2.00), O4 = 2.05 (2.00), O5 = 1.82 (2.00).

Experimental

Single crystals of ε-CaTe$_2$O$_5$ were obtained in small amounts by hydrothermal treatment of α-CaTeO$_3$ as starting material. α-CaTeO$_3$ (Stöger *et al.*, 2008) was prepared by the solid-state reaction of stoichiometric amounts of CaO and TeO$_2$ in evacuated fused silica ampoules at 973 K for 70 h. The reaction products obtained by this method contained small quantities (*ca* 3%) of the mixed-valence phase Ca$_4$Te$_5$O$_{14}$ (Weil, 2004). A 5 ml Teflon inlay was filled with the polycrystalline α-CaTeO$_3$ product (100 mg) and deionized water (3 ml), placed in a steel autoclave and heated at 493 K for 7 d. The residue was washed with water, ethanol and acetone. It consisted mainly of the unchanged polycrystalline α-CaTeO$_3$ phase and a few colourless crystals with undefined habit of the title compound.

Crystal data

CaTe$_2$O$_5$
M_r = 375.28
Monoclinic, $P2_1/c$
a = 9.382 (2) Å
b = 5.7095 (14) Å
c = 11.132 (3) Å
β = 115.109 (4)°
V = 540.0 (2) Å^3
Z = 4
Mo $K\alpha$ radiation
μ = 11.68 mm^{-1}
T = 293 (2) K
0.07 × 0.04 × 0.02 mm

Data collection

Bruker APEX CCD diffractometer
Absorption correction: multi-scan *SADABS* (Bruker, 2002)
$T_{\min}$ = 0.495, $T_{\max}$ = 0.800
5694 measured reflections
1569 independent reflections
1352 reflections with $I > 2\sigma(I)$
$R_{\rm int}$ = 0.039

Refinement

$R[F^2 > 2\sigma(F^2)]$ = 0.035
$wR(F^2)$ = 0.079
S = 1.07
1569 reflections
73 parameters
$\Delta\rho_{\max}$ = 1.96 e Å^{-3}
$\Delta\rho_{\min}$ = −1.15 e Å^{-3}

Table 1
Selected geometric parameters (Å, °).

Ca—O1$^{\rm i}$	2.305 (4)	Te1—O1	1.852 (4)
Ca—O2$^{\rm ii}$	2.326 (5)	Te1—O3	1.980 (5)
Ca—O2$^{\rm iii}$	2.358 (5)	Te1—O4	2.450 (5)
Ca—O1	2.360 (5)	Te2—O4$^{\rm iv}$	1.854 (4)
Ca—O3	2.476 (5)	Te2—O5	1.898 (4)
Ca—O4$^{\rm iii}$	2.554 (5)	Te2—O3	2.009 (5)
Ca—O4$^{\rm i}$	2.682 (5)	Te2—O5$^{\rm v}$	2.178 (5)
Te1—O2	1.832 (4)		
Te1—O3—Te2	123.4 (2)	Te2—O5—Te2$^{\rm v}$	103.5 (2)
Te2$^{\rm vi}$—O4—Te1	125.6 (2)		

Symmetry codes: (i) $-x, y+\frac{1}{2}, -z+\frac{3}{2}$; (ii) $-x, -y+1, -z+1$; (iii) $x, y+1, z$; (iv) $x, -y+\frac{1}{2}, z-\frac{1}{2}$; (v) $-x+1, -y+1, -z+1$; (vi) $x, -y+\frac{1}{2}, z+\frac{1}{2}$.

The highest remaining peak in the final difference Fourier map is located 0.75 Å from Te2 and the deepest hole is 2.01 Å from O5.

Data collection: *SMART* (Bruker, 2002); cell refinement: *SAINT* (Bruker, 2002); data reduction: *SAINT*; program(s) used to solve structure: *SHELXS97* (Sheldrick, 2008); program(s) used to refine structure: *SHELXL97* (Sheldrick, 2008); molecular graphics: *ATOMS* (Dowty, 2006); software used to prepare material for publication: *SHELXL97*.

Financial support from the FWF (Fonds zur Förderung der wissenschaftlichen Forschung), project No. P19099-N17, is gratefully acknowledged.

Supplementary data for this paper are available from the IUCr electronic archives (Reference: IZ3054). Services for accessing these data are described at the back of the journal.

References

Brese, N. E. & O'Keeffe, M. (1991). *Acta Cryst.* B**47**, 192–197.
Brown, I. D. (2002). *The Chemical Bond in Inorganic Chemistry: The Bond Valence Model*. Oxford University Press.
Bruker (2002). *SMART*, *SAINT* and *SADABS*. Bruker AXS Inc., Madison, Wisconsin, USA.
Dolgikh, V. A. (1991). *Russ. J. Inorg. Chem.* **36**, 1117–1129.
Dowty, E. (2006). *ATOMS for Windows*. Version 6.3. Shape Software, Kingsport, Tennessee, USA.
Gorbenko, V. M., Kudzin, A. Yu. & Sadovskaya, L. Ya. (1983). *Izv. Akad. Nauk SSSR Neorg. Mater.* **19**, 295–298.
Hanke, K., Kupčik, V. & Lindqvist, O. (1973). *Acta Cryst.* B**29**, 963–970.
Hottentot, D. & Loopstra, B. O. (1979). *Acta Cryst.* B**35**, 728–729.
Johnston, M. G. & Harrison, W. T. A. (2002). *Acta Cryst.* E**58**, i59–i61.
Miletich, R. (1993). *Mineral. Petrol.* **48**, 129–145.
Mishra, R., Namboodiri, P. N., Tripathi, S. N. & Dharwadkar, S. R. (1998). *J. Alloys Compd*, **280**, 56–64.
Platte, C. & Trömel, M. (1981). *Acta Cryst.* B**37**, 1276–1278.
Redman, M. J., Chen, J. H., Binnie, W. P. & Mallo, W. J. (1970). *J. Am. Chem. Soc.* **53**, 645–648.
Sadovskaya, L. Ja., Dudnik, E. F., Kudzin, A. Ju. & Grzhegorzhevskii, O. A. (1987). *Ferroelectrics*, **76**, 117–122.
Sadovskaya, L. Ja., Dudnik, E. F., Scherbina, S. A. & Grzhegorzhevskii, O. A. (1983). *Ferroelectrics*, **48**, 109–112.
Shannon, R. D. (1976). *Acta Cryst.* A**32**, 751–767.
Sheldrick, G. M. (2008). *Acta Cryst.* A**64**, 112–122.
Stöger, B., Weil, M., Zobetz, E. & Giester, G. (2008). In preparation.
Tripathi, S. N., Mishra, R., Mathews, M. D. & Namboodiri, P. N. (2001). *Powder Diffr.* **16**, 205–211.
Trömel, M. & Ziethen-Reichnach, H. (1970). *Z. Anorg. Allg. Chem.* **378**, 232–237.
Weil, M. (2004). *Solid State Sci.* **6**, 29–37.
Weil, M. (2005). *Acta Cryst.* E**61**, i237–i239.
Zemann, J. (1971). *Monatsh. Chem.* **102**, 1209–1216.